Dynamics of Solar and Stellar Convection Zones and Atmospheres
Proceedings IAU Symposium No. 365, 2024
A. V. Getling & L. L. Kitchatinov, eds.
doi:10.1017/S1743921323004209

The effect of Coulomb interactions on acoustic oscillations in the outer layers of low-mass stars

Ana Brito[1,2] **and Ilídio Lopes Fuentes**[2]

[1]Instituto Superior de Gestão
Rua Prof. Reinaldo dos Santos 46, 1500-522, Lisbon, Portugal
email: anabrito@isg.pt

[2]Centro de Astrofísica e Gravitação - CENTRA, Departamento de Física, Instituto Superior Técnico, Universidade de Lisboa
Av. Rovisco Pais 1, 1049-001, Lisbon, Portugal
email: ilidio.lopes@tecnico.ulisboa.pt

Abstract. As is well known, low-mass stars constitute the most abundant class of stars in our galaxy. In stars less massive than the Sun, the density within stellar interiors increases as the stellar mass decreases. Therefore, for low-mass stars, the significance of electrostatic effects in stellar interiors cannot be neglected, as these interactions can alter the properties of matter.

In our study, we focus on exploring the outer layers of stars less massive than the Sun. We have computed a range of stellar models, ranging from 0.4 to 0.9 solar masses, to investigate the effects of two physical processes on the acoustic oscillations in the envelopes of these stars: partial ionization of chemical elements and electrostatic interactions between particles in the outer layers. In addition to partial ionization, we demonstrate that Coulomb effects also influence the acoustic oscillation spectrum. Our investigation reveals the following findings:

1. Coulomb effects can indeed influence the acoustic oscillations in low-mass stars.
2. The model with a mass of $0.6\,M_{\odot}$ serves as a transition point. For models less massive than $0.6\,M_{\odot}$, their acoustic spectrum is more affected by electrostatic interactions, whereas models more massive than $0.6\,M_{\odot}$ have their acoustic spectrum more impacted by partial ionization processes.

Our work unveils the promising possibilities that future discoveries related to the detection of solar-like oscillations in stars less massive than the Sun could offer in terms of understanding the connections between the internal structure of low-mass stars and their observable characteristics.

Keywords. Asteroseismology, Low-mass stars, Stellar interiors, Coulomb effects, Partial ionization

1. Introduction

It is known from observations that stellar formation mechanisms favor the creation of low-mass stars, which constitute the most abundant class of stars in our Milky Way Bochanski et al. (2010). Specifically, M dwarfs make up approximately 70% of the solar neighborhood. However, this class of stars is the least understood due to their faintness and complex atmospheres, making it challenging to obtain reliable observational data. These stars possess convective envelopes (or are fully convective) and therefore have the potential to exhibit solar-like oscillations. Nevertheless, only a limited number of stars less massive than the Sun have had solar-like oscillations detected, primarily due to the small amplitudes of these oscillations (Borucki et al. 2010 - *Kepler*). Nonetheless, efforts

to detect solar-like oscillations persist with upcoming missions such as PLATO (e.g., Rauer et al. 2014), ground-based initiatives like the Stellar Observations Network Group (Grundahl et al. 2017), and high-precision telescopes such as the Keck Planet Finder (Gibson et al. 2016).

It is well-known that as stellar masses decrease, the densities within their interiors increase. With increasing density in a stellar interior, we cannot disregard the electrostatic interactions between the particles comprising the stellar plasma. This is because electrostatic interactions between particles alter the properties of matter. For example, electrostatic interactions lead to a reduction in pressure and ionization potential, resulting in a physical process known as pressure ionization in the deeper layers of stars. Additionally, the electron shielding effect decreases the repulsion between nuclei, facilitating nuclear reactions. While electron conduction and crystallization are also possible phenomena, they are not applicable to the types of stars studied in this research.

In this study, we investigate the impact of electrostatic effects on the acoustic oscillation spectrum of six theoretical stellar models with masses ranging from $0.9\,M_{\odot}$ to $0.4\,M_{\odot}$. It's important to note that all these models have a radiative interior and a convective envelope. These models were computed using the stellar evolution code MESA (Paxton et al. 2011, 2013, 2015, 2018; Jermyn et al. 2019), and for calculating the adiabatic oscillation mode frequencies, we employed the stellar pulsation code GYRE (e.g., Townsend & Teitler 2013). Further details regarding the input physics of these models can be found in the source paper Brito & Lopes (2021).

In the next section, section 2, we describe the outer convective layers of the models using thermodynamic quantities. Then, in section 3, we analyse from a seismic point of view the outer layers of the six theoretical models. Lastly, our conclusions (section 4) will be presented, along with a preview of our forthcoming work, which also emphasizes the significance of electrostatic interactions, although in the internal radiative zones of low-mass stars.

2. The adiabatically stratified convective zones

In this section, we will explore the outer convective envelopes of the six theoretical models. To achieve this, we will examine the profiles of four thermodynamic quantities: the first adiabatic exponent, the acoustic potential, the sound speed gradient, and the plasma coupling parameter. It is well known that the convective envelopes of low-mass stars exhibit a quasi-adiabatic stratification. The first adiabatic exponent, denoted as $\Gamma_1 = (\partial \ln P/\partial \ln \rho)_{ad}$, and represented in Figure 1, is determined by the equation of state and defines the structure of the adiabatic convective zones. As shown in Figure 1, the behavior of Γ_1 around its monoatomic ideal gas value is primarily influenced by two physical processes: partial ionisation of atomic species and electrostatic interactions between particles. An increase in the degree of ionization results in a decrease in Γ_1 (this is particularly evident in the ionization zones of light elements). Instead, electrostatic interactions between particles lead to an increase in the values of Γ_1.The first adiabatic exponent also plays a special role in asteroseismology. This is because, for acoustic oscillations, the adiabatic sound speed is determined by the equation $c^2 = \Gamma_1 P/\rho$.

In addition to Γ_1, another important quantity to investigate is the acoustic potential. By using the acoustic depth ($\tau = \int_r^R dr/c$) as an independent variable, which represents the wave's travel time from the star's surface to a specific radius depth r, we can describe the propagation of adiabatic acoustic oscillations in the outer layers of low-mass stars using a Schrödinger-type equation: $d^2\psi/d\tau^2 + (\omega^2 - U^2)\psi = 0$. Here, ω represents the angular frequency of the acoustic mode, and U^2 denotes the acoustic potential. This quantity, the acoustic potential, is intricately linked to the thermodynamics of stellar

https://doi.org/10.1017/S1743921323004209 Published online by Cambridge University Press

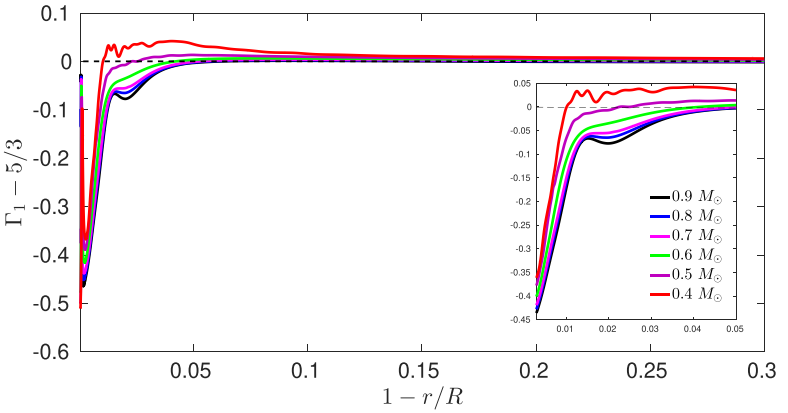

Figure 1. The first adiabatic exponent, Γ_1 is plotted for the outer layers of the six theoretical models.

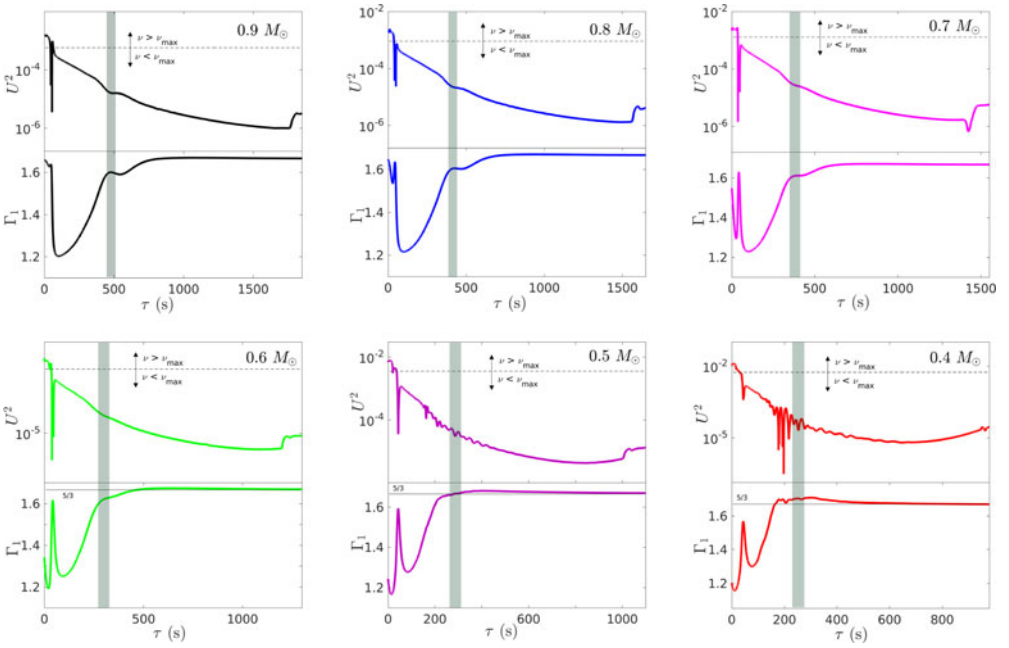

Figure 2. The acoustic potentials are plotted as functions of the acoustic depth in the upper layers of the theoretical models (upper panels). For comparison, Γ_1 is also represented as a function of the acoustic depth (lower panels).

interiors and is influenced by physical processes such as partial ionization of chemical elements and Coulomb interactions between particles. There is another compelling reason why the acoustic potential holds great significance, which will become evident in the upcoming Section 3. Figure 2 illustrates the acoustic potentials plotted as functions of acoustic depth for all six models. In the case of more massive models, the dip corresponding to helium ionization is clearly visible. However, for the $0.6\,M_\odot$ model, this dip nearly vanishes due to the increasing importance of electrostatic effects. Finally, in the less massive models, a distinct noisy pattern is observable, reflecting the impact of electrostatic interactions between charged particles.

https://doi.org/10.1017/S1743921323004209 Published online by Cambridge University Press

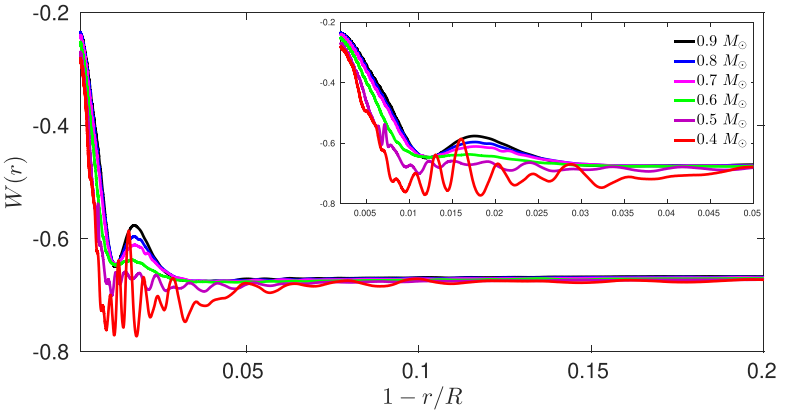

Figure 3. The sound-speed gradient, W is plotted for the outer layers of the six theoretical models.

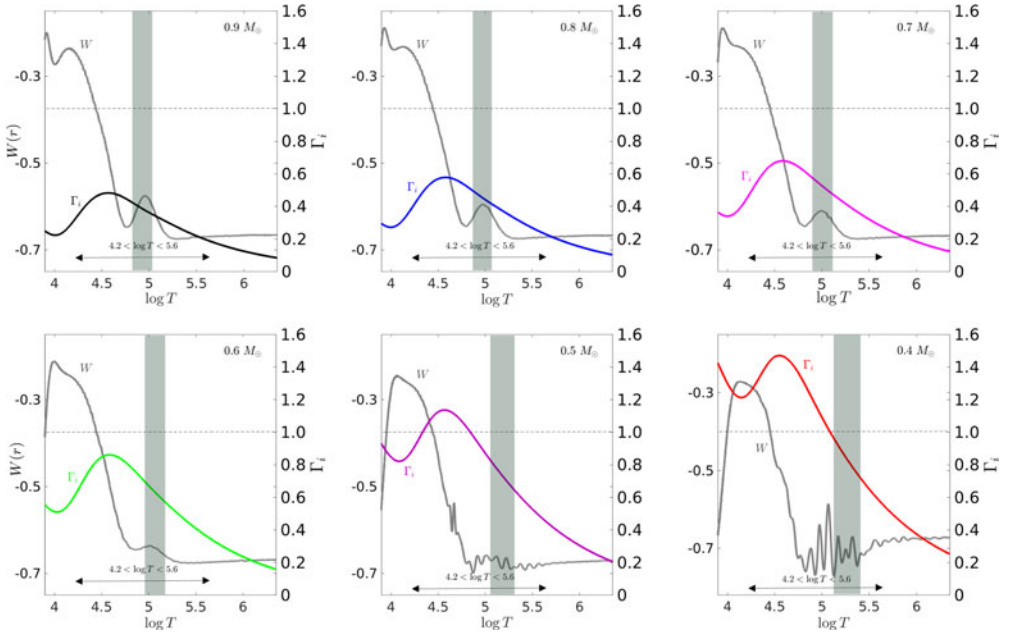

Figure 4. The ionic plasma coupling parameter, Γ_i, is plotted as a function of temperature for all six theoretical models. The temperature range $4.2 \lesssim \log T \lesssim 5.6$ is especially important for electrostatic interactions because it contains the intervals where the two helium ionisations occur. Additionally, we have overlaid the sound-speed gradient profiles in grey for comparison.

Another diagnostic quantity that is sensitive to Γ_1 is the sound speed gradient represented in figure 3 for all the six models. Here as well, we observe that the perturbations in the acoustic spectrum of more massive stars are more affected by partial ionization processes, resulting in a moderate variation in the sound speed gradient. In contrast, for less massive models, the acoustic spectrum is more influenced by electrostatic interactions, leading to a pronounced oscillatory component in the profile of the sound speed gradient.

To complete the study of the convective outer layers of the models, we also computed the plasma coupling parameter. The plasma parameter represents the ratio of the average potential energy to the thermal kinetic energy of the gas. Figure 4 illustrates the plasma

https://doi.org/10.1017/S1743921323004209 Published online by Cambridge University Press

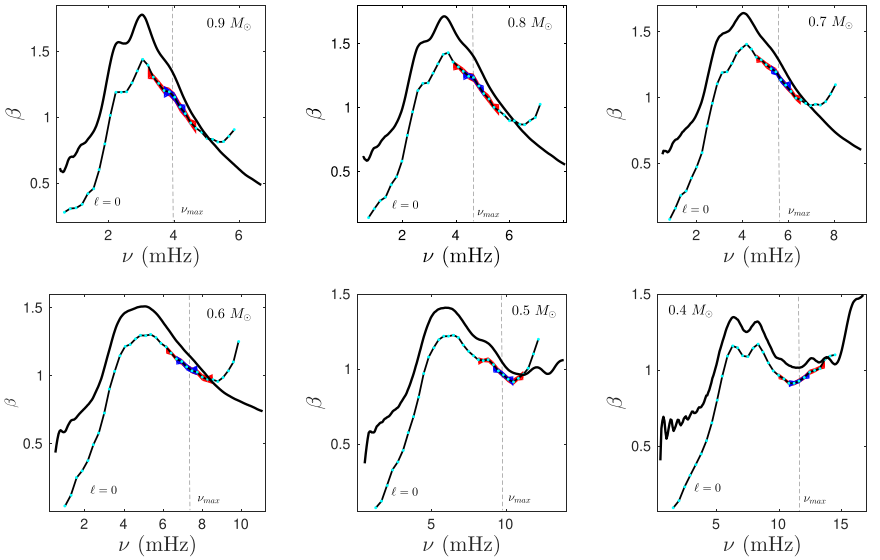

Figure 5. The seismic diagnostic β is numerically computed from the structural model parameters (indicated by the solid, thicker black line). The thinner, solid black line represents the diagnostic β computed from a theoretical table of frequencies ($\ell = 0$), with the mode frequencies highlighted in cyan. In this figure, two shaded regions are shown: one in blue and the other in red. These regions result from tests that validate the stability of the algorithm.

interaction parameter plotted within the temperature range where the two helium ionisations occur, which is also the temperature range where Coulomb effects are known to be more significant. The value of the plasma parameter increases as stellar mass decreases. Moreover, for the less massive stellar models, the plasma parameter value is above one or close to one in this temperature range. This suggests that the strong oscillatory signal in the sound speed gradient can indeed be attributed to Coulomb effects.

3. Seismic analysis of the outer layers

Helio- and asteroseismology have demonstrated that abrupt variations in the sound speed produce a quasi-periodic oscillatory component in the frequencies of stellar acoustic oscillations (e.g., Gough & Toomre 1991). This type of signal contains information that helps in our understanding of the physical processes taking place within stellar interiors. In this section, we will analyse the outer layers of the six theoretical models from a seismic perspective. To accomplish this, we will employ a seismic diagnostic denoted as β, which is particularly suited for studying the outer convective layers of low-mass main-sequence stars (e.g., Brodskii & Vorontsov 1987; Vorontsov & Zharkov 1989; Brito & Lopes 2019, 2018). In the previous section, when we introduced the concept of the acoustic potential, we mentioned that the acoustic potential is of interest for two primary reasons. The second reason will now become clear, and it is as follows: we can establish a connection between the shape of the acoustic potential and the shape of the seismic diagnostic β. Figure 5 illustrates the seismic diagnostic $\beta(\nu)$, where ν represents the cyclic frequency, numerically computed from the structural model parameters (indicated by the thicker black solid line) for all the models. The quasi-periodic signal in $\beta(\nu)$ observed in the more massive models (0.9, 0.8, and 0.7 $M_\odot$) is associated with the dip in the acoustic potential found in the region of partial ionization of light elements, specifically the second helium ionization. The 0.6 $M_\odot$ model serves as a transitional model in the sense that the quasi-periodic oscillations linked to helium ionization completely disappear. For models

https://doi.org/10.1017/S1743921323004209 Published online by Cambridge University Press

less massive than $0.6\,M_{\odot}$, the shape of the seismic diagnostic $\beta(\nu)$ is entirely different from that of $\beta(\nu)$ for the more massive models, reflecting the significance of electrostatic interactions between particles in the acoustic spectrum. Figure 5 also presents the seismic parameter $\beta(\nu)$ obtained from theoretical tables of mode frequencies for each model. These frequencies were computed using the stellar pulsation code GYRE (e.g., Townsend & Teitler 2013).

The frequencies near ν_{max} are of particular interest because it is in the vicinity of this value that the detection of observational modes of oscillation is more likely. If we consider a local linear approximation in the vicinity of ν_{max}, we observe that as the significance of Coulomb effects increases, the slope of the line changes, allowing us to differentiate between the cases. It is evident that the diagnostic potential of β significantly improves with the number of modes used in its calculation. However, even with only five modes per degree, the behavior of β for a $0.9\,M_{\odot}$ star can be distinguished from that of a $0.4\,M_{\odot}$ star (see figure 5).

4. Conclusions

In this study, we investigate the oscillatory patterns present in the oscillation mode frequencies of six theoretical low-mass main-sequence stellar models ($0.4\,M_{\odot} < M < 0.9\,M_{\odot}$), resulting from two distinct physical processes: the partial ionization of light elements and the electrostatic interactions between the particles constituting the stellar plasma.

The $0.6\,M_{\odot}$ stellar model serves as a reference model, with models more massive than $0.6\,M_{\odot}$ having their acoustic spectrum primarily influenced by partial ionization processes, while models less massive than $0.6\,M_{\odot}$ have their acoustic spectrum predominantly affected by Coulomb effects. Therefore, this work unveils the potential for future discoveries related to the detection of solar-like oscillations in stars less massive than the Sun to provide insights into the study of the relationships between the internal thermodynamics of low-mass stars and their observable characteristics.

Finally, we would like to emphasize that the interiors of low-mass stars constitute what is commonly referred to as a hot and dense plasma. By definition, a plasma is associated with two key concepts: the concept of quasi-neutrality and the concept of collective behavior. Quasi-neutrality implies that the plasma maintains an overall neutral charge, but it is not so neutral that all the significant electromagnetic forces disappear (e.g., Chen 2016). This means that stellar interiors can exhibit small local imbalances of electric charge. Consequently, the study of the electrostatic properties of stellar interiors holds great potential for enhancing our understanding of the observable patterns of rotation and magnetic activity in low-mass main-sequence stars.

References

Bochanski, J., Hawley, S., Covey, K., *et al.* 2010, *AJ*, 30, 490
Borucki, W., Koch, D., Basri, G., *et al.* 2010, *Science* 377, 977
Brito A. & Lopes I. 2018, *ApJ* 853, 183
Brito A. & Lopes I. 2019, *MNRAS* 488, 1558–1571
Brito A. & Lopes I. 2021, *MNRAS* 507, 5747–5757
Brodskii M. & Vorontsov S. 1987, *SvAL* 13, 179
Chen, F. 2016, *Introduction to Plasma Physics and Controlled Fusion*
Gibson, S., Howard, A., Marcy, G., *et al.* 2016, *Society of Photo-Optical Instrumentation Engineers (SPIE) Conference Series* 9908, 990870
Gough D. & Toomre J. 1991, *ARAA* 29, 627–684
Grundahl, F., Fredslund Andersen, M., Christensen–Dalsgaard, J., *et al.* 2017, *ApJ* 836, 142
Jermyn, A., Bauer, E., Schwab, J., *et al.* 2019, *ApJS* 265, 15

https://doi.org/10.1017/S1743921323004209 Published online by Cambridge University Press

Paxton, B., Bildsten, L., Dotter, A., *et al.* 2011, *ApJS* 192, 3
Paxton, B., Cantiello, M., Arras, P., *et al.* 2013, *ApJS* 208, 4
Paxton, B., Marchant, P., Schwab, J., *et al.* 2015, *ApJS* 220, 15
Paxton, B., Schwab, J., Bauer, E., *et al.* 2018, *ApJS* 234, 34
Paxton, B., Smolec, R., Schwab, J., *et al.* 2019, *ApJS* 243, 10
Rauer, H., Catala, C., Aerts, C., *et al.* 2014, *Experimental Astronomy* 38, 249–330
Townsend, R. & Teitler, S. 2013, *MNRAS* 435, 3406–3418
Vorontsov, S. & Zharkov, V. 1989, *APSPR* 13, 179

https://doi.org/10.1017/S1743921323004209 Published online by Cambridge University Press